

# The Effect of Anode Chloride Contents in Macro-Cell Corrosion

Gaozai Xu, Makoto Hibino\*, Hiroki Goda and Zhonglu Cao

Concrete laboratory in department of Civil Engineering, Kyushu Institute of Technology, Kitakyushu-shi,804-8550, Japan

## Abstract

This research recorded the polarization process of chloride-induced macro-cell corrosion and polarization ratios and slopes are utilized to reveal the macro-cell corrosion mechanism. The results indicate anode chloride contents can increase macro-cell current density, and only if the corrosion can be initiated, lower chloride content can also increase current density if entered into later corrosion period. Moreover, with the deteriorating of chloride-induced corrosion, macro-cell corrosion will be more controlled by cathode, and anode will lose its control progressively. Additionally, increasing of anode chloride contents in anode can increase macro-cell potential difference and decrease anode polarization resistance but cannot affect cathode polarization resistance, and enlarging of macro-cell potential difference and decreasing of anode polarization resistance are the key determinant of escalating of macro-cell current density.

**Keywords:** Macro-Cell Corrosion, Rebar, Chloride, Polarization Slope, Polarization Ratio

## 1. Introduction

Annually, 3% of world GDP is consumed by corrosion. Moreover, concrete construction consumes a large quantity of steel and the attention to rebar corrosion should not be ignored.

The corrosion status can be categorized into 2 types, namely micro-cell corrosion and macro-cell corrosion, and the distance between passive area and active area which is named anode and cathode can be used to classify these 2 types of corrosion<sup>[1]</sup>. In micro-cell corrosion status, anode and cathode are adjacent, which means they coexist in the same area along the rebar<sup>[2],[3]</sup> and this tends to be occurred in carbonation concrete or very high chloride content concrete. In macro-cell corrosion status, the distance between cathode and anode is further than micro-cell status<sup>[2]</sup> which means they are separated and this tends to be occurred in chloride-induced pitting corrosion (anode is tiny compared to the whole rebar) or the condition that cathode and anode are in different environment<sup>[1]</sup> such as the condition that only part of rebar is embedded in concrete and another part is outside of the concrete.

In chloride-induced corrosion, pitting corrosion tends to be occurred easily. Moreover, in the whole reaction, Cl<sup>-</sup> will not be consumed<sup>[4]</sup>, which means it acts as catalyst in

the whole process, so some authors<sup>[5]</sup> described it as “a specific and unique destroyer” which will cause macro-cell corrosion and serious deterioration.

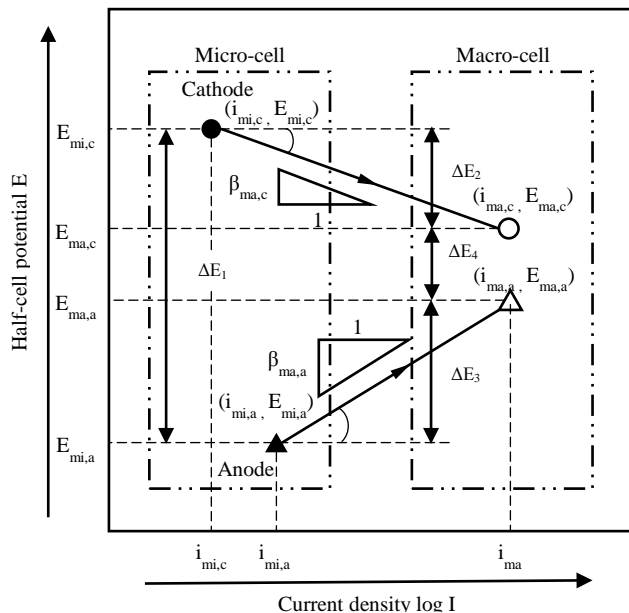


Fig. 1 Macro-cell corrosion model

After the generation of macro-cell, the separate electrodes will reach stable<sup>[6]</sup>. The corrosion can be illustrated in Fig. 1. Here, the polarization slope ( $\beta_{ma,c}$  and  $\beta_{ma,a}$ ) can reveal the macro-cell corrosion polarization ability of cathode and anode which can be applied in analysis. Specifically, the lower the cathode polarization slope is, the stronger the electrons to be consumed by cathode, which means lower polarization resistance in cathode, and the lower the anode polarization slope is, the stronger the electrons to be generated in anode, which means lower polarization resistance in anode. The calculation equation of polarization slope ( $\beta_{ma,c}$  and  $\beta_{ma,a}$ ) is as follows:

$$\beta_c = \frac{E_{mi,c} - E_{ma,c}}{i_{mi,c} - i_{ma,c}} \quad (1)$$

$$\beta_a = \frac{E_{mi,a} - E_{ma,a}}{i_{mi,a} - i_{ma,a}} \quad (2)$$

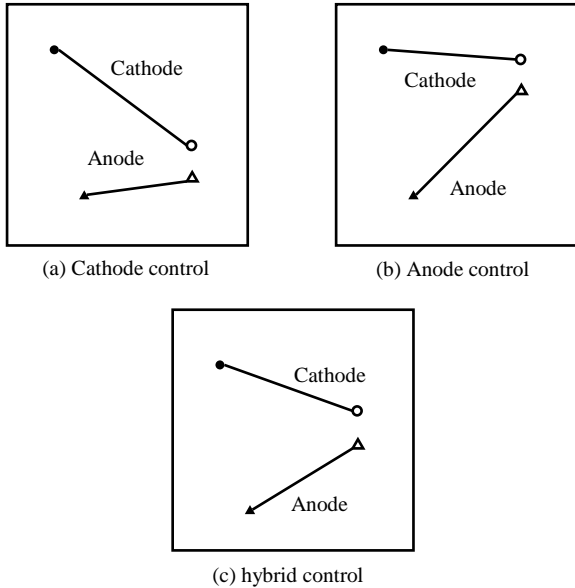


Fig. 2 Control mode of Macro-cell corrosion

Moreover, polarization ratio is another index to distinguish whether the macro-cell corrosion is cathode control or anode control or hybrid control [7], which is illustrated in Fig. 2 and the polarization ratio can be defined as follows:

$$PR_c = \frac{\Delta E_2}{\Delta E_1} = \frac{E_{mi,c} - E_{ma,c}}{E_{mi,c} - E_{mi,a}} \quad (3)$$

$$PR_a = \frac{\Delta E_3}{\Delta E_1} = \frac{E_{ma,a} - E_{mi,a}}{E_{mi,c} - E_{mi,a}} \quad (4)$$

$$PR_r = \frac{\Delta E_4}{\Delta E_1} = \frac{E_{ma,c} - E_{ma,a}}{E_{mi,c} - E_{mi,a}} \quad (5)$$

$PR_c$ ,  $PR_a$  and  $PR_r$  mean the control content of cathode, anode and resistance which can be utilized to evaluate the control mode. At the situation that  $PR_c$  is quite higher than  $PR_a$  and  $PR_r$ , which means anode can prove enough electrons and will not be the main reason to affect the corrosion. Here, the macro-cell is controlled by cathode mainly and happens in the condition with ample chloride contents in anode, which can be named cathode control illustrated in Fig. 2 (a). At the situation that  $PR_a$  is quite higher than  $PR_c$  and  $PR_r$ , which means cathode can consume enough electrons and will not be the main reason to affect the corrosion. Here, the macro-cell is controlled by anode mainly and happens in the condition with enough oxygen or hydrogen ion in cathode, which can be named anode control illustrated in Fig. 2 (b); At the situation that both  $PR_a$  and  $PR_c$  are quite high and equal with each other approximately, and are quite higher than  $PR_r$ , which means anode can prove enough electron to be consumed by anode. Here, the macro-cell is controlled by cathode and anode together, namely, hybrid control illustrated in Fig. 2 (c).

Many research concerning chloride-induced corrosion is based on micro-cell, which means cathode and anode are coexisted and research concerning macro-cell hasn't been focused significantly. Ominda Nanayakkara and Yoshitaka Kato [8] analyzed different chloride concentration and had the conclusion that macro-cell corrosion will be easily occurred in high chloride region and even uniform chloride content along rebar, macro-cell can be formed as well. Even so, these work didn't pay enough attention to the macro-cell polarization behavior. So this research will analysis the macro-cell corrosion through polarization ratios and slopes to reveal the macro-cell corrosion mechanism.

## 2. Experiment Summary

### 2.1 Experiment design

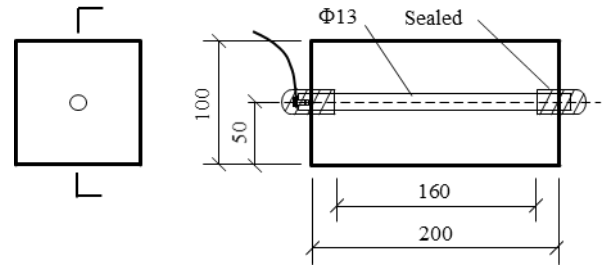


Fig. 3 Cathode and Anode specimen

Table 1 The Composition of Cathode and Anode

Case	Cathode	Anode	$\Delta Cl/wt\%$
	CL/wt%	CL/wt%	
1	1.5	3.0	1.5
2	1.5	4.5	3.0
3	1.5	6.0	4.5

Plain round mild rebar 13 mm in diameter and 220mm in length is embedded in mortar in the experiment. The specimen sizes of cathode and anode are illustrated in Fig. 3. The protective film of the certain corrosion area is removed by sand paper, and then other area of the rebar is wrapped with heat shrink tubes ( $\Phi=19.1mm$ ). After that the rebar is put into oven with the heat shrink tube, and it will be taken out after shrunk. In the cooling condition the junctions between rebar and heat shrink tube are cover with a layer of polystyrene resin to ensure it air tight and water tight. Additionally, in one of the ends, a lead wire is connected to the rebar through a screw ( $\Phi=4mm$ ). Moreover, the composition of cathode is demonstrated in Table 1 in detail. The effective corrosion length of rebar in cathode and anode are both 160 mm, and the chloride

content is 1.5 wt% (by weight of cement) in cathode, but the chloride contents in anode are 3.0 wt%, 4.5 wt% and 6.0 wt% respectively. The mix proportion of the whole experiment is 0.5:1:3(water: cement: sand). The cement is ordinary Portland cement with density of 3.15 g/cm<sup>3</sup> and the sand is washed before passing from sieve (4.75mm) with the density of 2.59 g/cm<sup>3</sup> after water absorption. The chloride is from NaCl and the purity is above 99%, which is dissolved with water before casting. All the specimens were set in molds for 1 days before being demolded and then were cured in the water for 2 weeks. After that they were put into the curing chamber for another 2 weeks before measurement.

### 2.2 Experiment measurement

The experiment was done for 8 cycles (112 days) and the data was recorded every day, which is demonstrated in Fig. 4. There are 2 periods, namely, separated period and connected period during the experiment and both periods consume 1 week. In separated period micro-cell potential ( $E_{mi,c}$  and  $E_{mi,a}$ ) and current density ( $i_{mi,c}$  and  $i_{mi,a}$ ) can be obtained and in connected period, macro-cell potential ( $E_{ma,c}$  and  $E_{ma,a}$ ) and current density ( $i_{cor}$ ) can be obtained. Then the polarization curve can be obtained according to the paper of Tsuyoshi Maruya et al<sup>[6]</sup> which

has been illustrated previously.

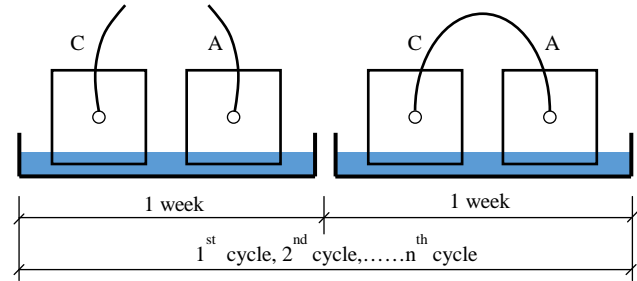


**Fig. 4** The cycle process of experiment

During the experiment, machine CM-SE1 is used to measure half-cell potential ( $E_{mi,c}$ ,  $E_{mi,a}$ ,  $E_{ma,c}$  and  $E_{ma,a}$ ) and resistance of rebar ( $R_p$ ), and the measure method refers to standard ASTM C876<sup>[9]</sup>. Moreover, the micro-cell corrosion current density ( $i_{mi,c}$  and  $i_{mi,a}$ ) is calculated by Stern-Geary equation:  $I_{cor,mi} = B/R_p$ ,  $B = \beta_a \beta_c / [2.3(\beta_a + \beta_c)]$ . In the formula,  $\beta_a$ ,  $\beta_c$  means Tafel constant of anode and cathode,  $R_p$  means rebar polarization resistance and  $B$  means Stern-Geary constant. In the environment of concrete, 26mv can be used in corroded status and 52 mv in passivation status to represent the constant  $B$ <sup>[10],[11],[12]</sup>.

Moreover, zero resistance ammeter is used to measure the macro-cell current ( $I_{ma}$ ) at connected period. The current density is calculated by equation:  $i_{ma} = I_{ma}/A_a$ . In

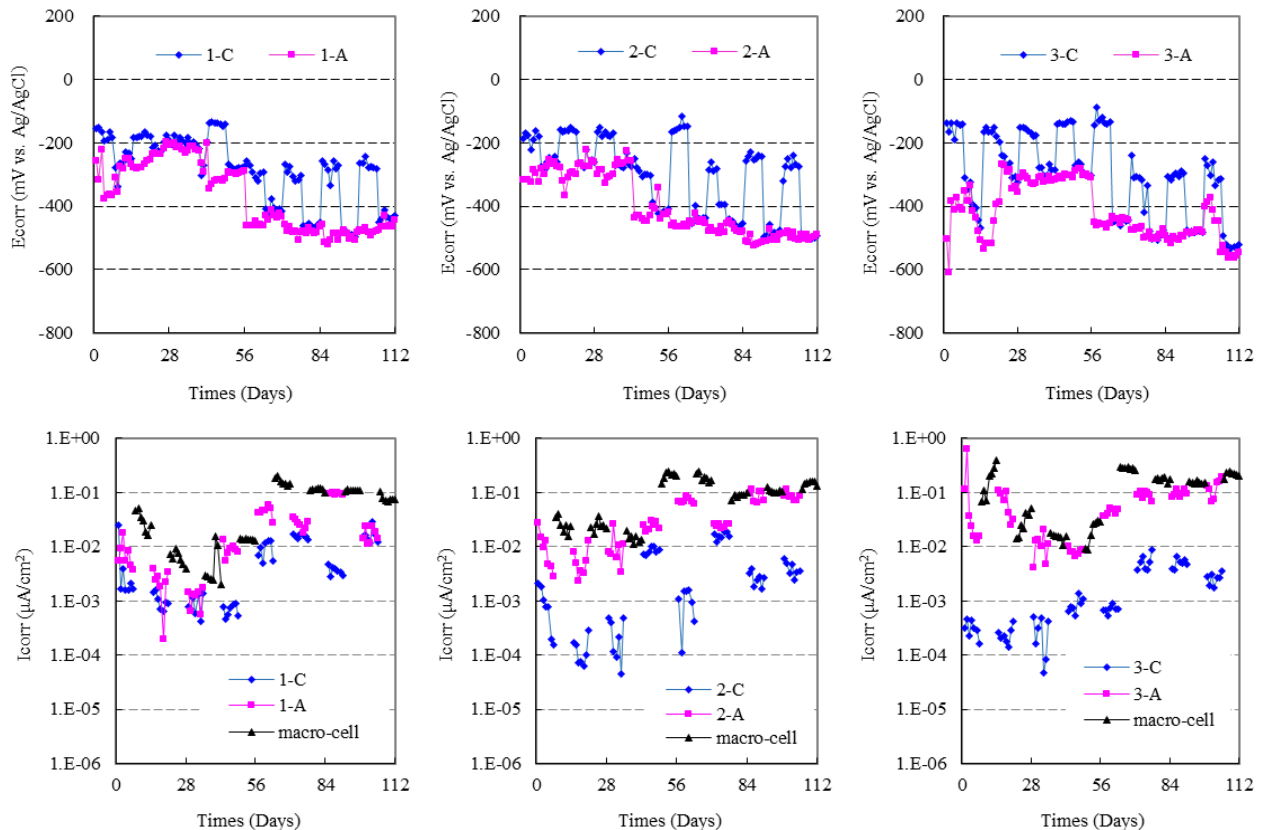


**Fig. 5** Time evaluation curve of half-cell potential, micro-cell current density, macro-cell current density in each case

the equation,  $A_a$  means the effective anode rebar surface area.

### 3. Result and Analysis

#### 3.1 Time evaluation curve of $E_{corr}$ , $i_{corr}$

The time evaluation curves of half-cell potential, micro-cell current density and macro-cell current density of Case 1, 2 and 3 demonstrated in Table 1 are illustrated in Fig. 5. As a whole, in every cycle, almost all the data fluctuated in a limited range, specifically, all the curves gradually tend to be stable after the several initial cycles (1-4 cycle) and with the processing of corrosion, the half-cell potential differences in separated period enlarge dramatically and finally tend to be stable, which may be due to the deterioration of corrosion. Moreover, almost all of the half-cell potentials are between -150mV and -600mV, and compared with anode, the half-cell potential of cathode in separated period is much more stable than anode. To see from a macroscopic perspective, the rebar with a higher potential (cathode) is considerably polarized to a lower level and the one with lower potential (anode) is subtly polarized to a higher level, which means the polarized potential of cathode and anode is more close to anode. This is mainly because the electrons from the anode rebar can go into cathode continually, which disturbs the original polarization condition. In the aspect of current density, the macro-cell current density is more close to the current density of anode especially in Case 2 and 3 and after 4 cycles the macro-cell current density becomes comparatively stable.

What should be recognized is that the time evaluation curve can only dedicate a whole view of the experiment result and afford an analysis basis. According to the analysis, the processing of macro-cell corrosion should be divided into 2 periods to get the precise conclusion, namely, initial corrosion period (1-4 cycle) and later corrosion period (5-8 cycle).

#### 3.2 Effect of anode chloride contents on macro-cell current density

To evaluate the corrosion degree of macro-cell corrosion, macro-cell current density is one of the significant parameter and the influence factors including macro-cell potential differences, cathode polarization slope and anode polarization slope. Here, macro-cell current density will be analyzed initially, and the relationship between macro-cell current density ( $I_{ma}$ ) and chloride difference ( $\Delta Cl^-$ ) between cathode and anode is illustrated in Fig. 6, where the separated 2 periods, namely, initial

corrosion period (1-4 cycle) and latter corrosion period (5-8 cycle) are illustrated as well.

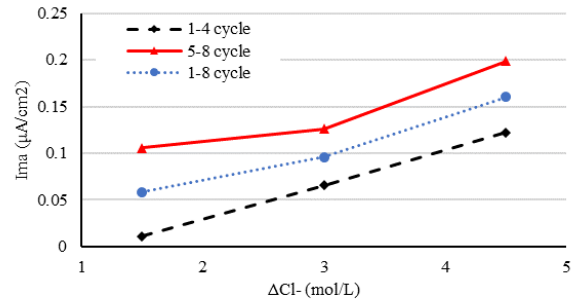


Fig. 6 The relationship between  $I_{ma}$  and  $\Delta Cl^-$

As a whole, in the entire corrosion process (1-8 cycle), the average macro-cell current density of Case 1, 2 and 3 are 0.058, 0.096 and 0.160  $\mu A/cm^2$  respectively, which surges noticeably with the gradually creeping up of chloride difference between cathode and anode from 1.5 to 4.5wt%. Once the 2 corrosion periods are separated, the anode macro-cell current density is separated as well. In initial corrosion period, the current density is 0.011, 0.065 and 0.122  $\mu A/cm^2$  respectively, and in latter corrosion period, the current density is 0.105, 0.126 and 0.199  $\mu A/cm^2$  respectively in Case 1, 2 and 3. Specifically, in Case 3 although in initial corrosion period the macro-cell current density is higher than 0.1  $\mu A/cm^2$ , which means high chloride difference between cathode and anode can initiate corrosion easily and form macro-cell corrosion quickly. Additionally, in latter corrosion period, all of the macro-cell current density in each case is higher than 0.1  $\mu A/cm^2$ , which means even though lower chloride difference exists between cathode and anode, serious corrosion can be generated in latter corrosion period only if the corrosion can be initiated.

#### 3.3 Effect of anode chloride contents on macro-cell potential difference

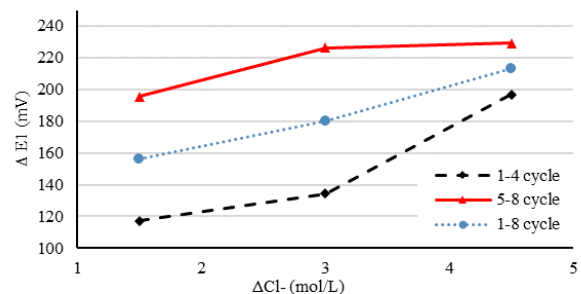


Fig. 7 The relationship between  $\Delta E_1$  and  $\Delta Cl^-$

Through the analysis above, the deterioration of corrosion tends to be generated with the creeping up of chloride difference contents between cathode and anode, and as the driving force of macro-cell corrosion, the macro-cell potential difference cannot be neglected.

Macro-cell potential difference ( $\Delta E_1$ ) of the entire corrosion process (1-8 cycle), initial corrosion period (1-4 cycle) and later corrosion period (5-8 cycle) are illustrated in Fig. 7. As to the entire corrosion process,  $\Delta E_1$  of Case 1, 2 and 3 are 156.38, 180.34 and 213.06mV respectively, which means with the generally creeping up of  $\Delta Cl^-$ ,  $\Delta E_1$  eases up continuously as well, which may be one of the reasons for the increasing of macro-cell current density. When separated,  $\Delta Cl^-$  of the 2 periods are separated clearly as well in the figure. In initial corrosion period,  $\Delta E_1$  of each case is 117.10, 134.25, and 197.00mV respectively and in later corrosion period is 195.67, 226.42 and 229.12 mV respectively. Compared with Case 3,  $\Delta E_1$  of Case 1 and 2 climbs significantly, which means although the chloride contents difference between cathode and anode are not high, the macro-cell potential difference can reach a high level in the later corrosion period.

### 3.4 Effect of anode chloride contents on polarization ratios

Corrosion ratio reflects the control mode of the

corrosion and  $PR_c$ ,  $PR_a$  and  $PR_r$  of each case is illustrated in Fig. 8 (1-8 cycle). and the whole data is divided into 2 periods as well which is illustrated in Fig. 8 (1-4 cycle) and Fig. 8 (5-8 cycle). In the entire corrosion process,  $PR_c$  of Case 1, 2 and 3 is 0.59, 0.78 and 0.88 respectively,  $PR_a$  is 0.31, 0.16 and 0.09 respectively and  $PR_r$  is 0.10, 0.09 and 0.09 respectively. Through the data, what can be realized is that the gradually creeping up of anode chloride contents have the effect not only on anode polarization ratio but also on cathode polarization and mortar resistance polarization ratio, especially cathode polarization ratio. Specifically, it causes the dramatically plummeting of anode polarization ratio, smoothly surging of cathode polarization ratio and fluctuating of mortar polarization ratio.

Once initial corrosion period and later corrosion period are separated, the ratios separated dramatically as well. In initial corrosion period,  $PR_c$  of Case 1, 2 and 3 is 0.39, 0.72 and 0.78 respectively,  $PR_a$  is 0.49, 0.26 and 0.15 respectively and  $PR_r$  is 0.12, 0.06 and 0.14 respectively. The entire trends of  $PR_c$ ,  $PR_a$ , and  $PR_r$  are still unchanged, which means  $PR_c$  is creeping up,  $PR_a$  is

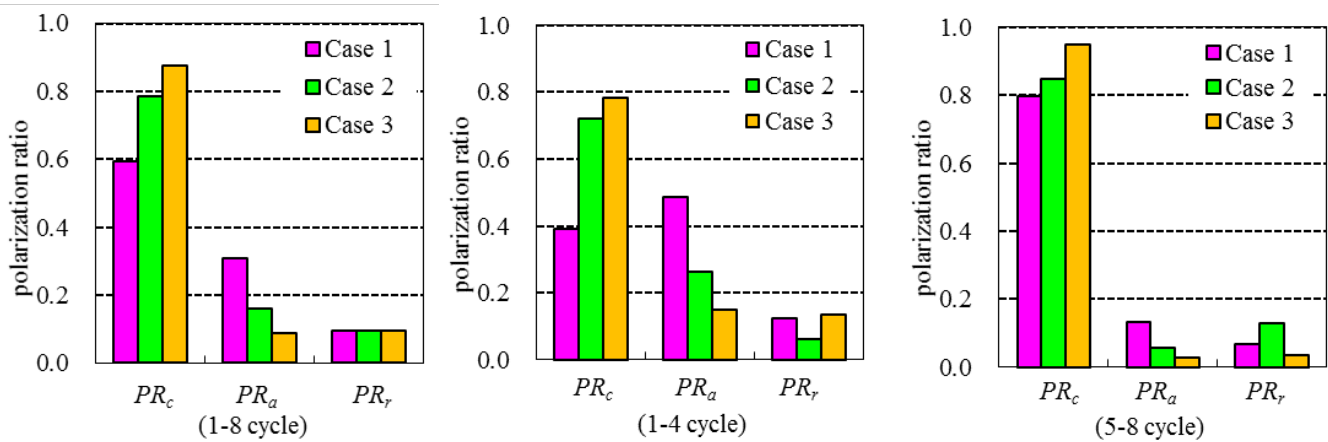


Fig. 8 Polarization ratios

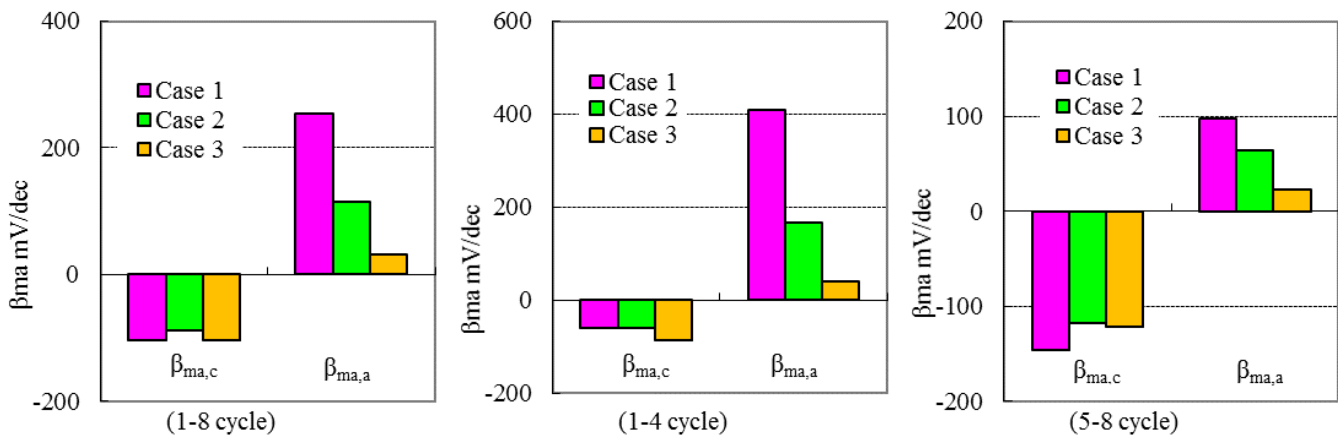


Fig. 9 Polarization slopes

creeping down and  $PR_r$  is fluctuating. The control mode of Case 1 is a hybrid control mode according to the theory introduced before, but Case 2 and Case 3 are anode control mode although in initial corrosion mode. Moreover, with the gradually creeping up chloride contents in anode, the cases are more controlled by anode. In later corrosion period,  $PR_c$  of Case 1, 2 and 3 is 0.80, 0.85 and 0.95 respectively,  $PR_a$  is 0.13, 0.06 and 0.03 respectively and  $PR_r$  is 0.07, 0.13 and 0.04 respectively. All cases are cathode control in later corrosion period and the control content is still increasing with the creeping up of chloride contents in anode. In addition, by comparing with the 2 periods, with the deterioration of corrosion aggravating, anode control content of every case increases to a higher level, especially in Case 1. This phenomenon can be explained by the generation electron that with the increasing of chloride difference between cathode and anode, the ability of anode to generate electron increases as well, which makes the macro-cell corrosion more controlled by the ability of cathode to consume the generated electron generated by anode. In addition, with the gradually creeping up of corrosion time, as the corrosion catalyst, chloride ion gathers in the surrounding of rebar, which can generate more electron to make the macro-cell be more controlled by cathode.

So, in both initial corrosion period and later corrosion period, the macro-cell corrosion will be more controlled by cathode with the creeping up of anode chloride content, and with the deterioration of corrosion, which means entered into later corrosion period, low chloride difference case can turn into cathode control mode as well.

### 3.5 Effect of anode chloride contents on polarization slopes

The main parameter to affect the macro-cell corrosion current density is macro-cell corrosion potential difference ( $\Delta E_1$ ), cathode polarization slope ( $\beta_{ma,c}$ ) and anode polarization slope ( $\beta_{ma,a}$ ), and  $\Delta E_1$  is one of the significant parameters in chloride-induced corrosion, which has already been analyzed and the remain 2 parameters should be analyzed as well. As introduced before polarization slopes are the significant parameters which can reveal the polarization ability of cathode and anode. So, firstly, the average polarization slopes of cathode and anode in all 8 cycles are illustrated in Fig. 9(1-8 cycle), where  $\beta_{ma,c}$  of cases 1, 2 and 3 with 3.0wt%, 4.5wt% and 6.0wt% chloride content in anode is -102.88, -88.28, and -104.11mV/dec respectively and  $\beta_{ma,a}$  is 253.38, 114.81 and 31.11mV/dec respectively. From the result, what is clear is that with the gradually creeping up of chloride content in anode,  $\beta_{ma,c}$  fluctuates between a certain range but  $\beta_{ma,a}$  will

dramatically plummet to a lower level. This means the anode chloride content has tremendous influence on the anode polarization slope, which can subside anode polarization resistance and then accelerate the macro-cell corrosion rate of rebar.

However, analyzing the initial corrosion period and latter corrosion period together may have the possibility to lose some significant information, so the separated 2 periods are illustrated in Fig. 9 (1-4 cycle) and Fig. 9 (5-8 cycle). In the initial corrosion period, the cathode polarization slope of each case is -59.97, -59.20 and -86.35mV/dec respectively and anode polarization slope is 408.64, 166.17 and 39.80mV/dec. In later corrosion period, the cathode polarization slope of each case is -145.80, -117.36 and -121.87mV/dec respectively and anode polarization slope is 98.11, 63.45 and 22.43mV/dec. By comparing with the 2 periods, with the increasing of corrosion time, the cathode polarization slope has a slightly easing up and the anode polarization slope has a slightly easing down especially in case 1 which drops from 408.64 to 98.11mV/dec. What should be noticed is that in later corrosion period all the absolute value of anode polarization slope is lower than initial corrosion period. This means increasing of chloride contents in anode and corrosion time can both reduce the reaction resistance in anode. Moreover, although cathode polarization slope remains fluctuating, the cathode polarization slope in the later corrosion period is higher than initial corrosion period in all cases.

So, the anode polarization slope will creep down to a lower level if the anode chloride content increases, or entered into later corrosion period. Although lower chloride content in anode, the anode polarization slope will be escalated to a lower level only if the macro-cell corrosion can be initiated.

## 4. Mechanism for anode chloride content to affect macro-cell corrosion

According to the analysis above, anode polarization ratio and slope is decreasing, and cathode polarization slope remains fluctuating with the creeping up of anode chloride contents. So this can be described in Fig 10 (a), which meets the result achieved by the analysis before. 1 means lower chloride difference ( $\Delta Cl^-$ ) between cathode and anode, and 2 represents higher  $\Delta Cl^-$ . It is quite clear that chloride has great effect on anode polarization curve and the increasing of macro-cell current density is mainly due to the enlarging of  $\Delta E_1$  and depolarization of anode.

Moreover, Fig. 10 (b) can be used to demonstrate the process from initial corrosion period to later corrosion period if assume 1 as initial corrosion and 2 as later corrosion period. When entered into later corrosion period, the anode will lose its control in macro-cell corrosion progressively. Specifically, cathode ratio and slope will increase to a higher level and anode ratio and slope will decrease to a lower level. It is clear that only if the corrosion can be initiated, with the deterioration of corrosion,  $\Delta E_1$  will be enlarged, and the anode polarization slope will be decreased to increase macro-cell current density.

### 4. Conclusions

Through the 8-cycles-experiment of macro-cell corrosion, the effect of chloride to macro-cell corrosion in initial and latter corrosion period can be concluded. With the creeping up of chloride difference between cathode and anode, macro-cell current density booms to a higher level, although in initial corrosion period, and once entered later corrosion, the current density will escalate to a high level as well only if the macro-cell can be initialed. Moreover, improving anode chloride contents or entering into later corrosion period, the macro-cell corrosion will be more controlled by cathode, and anode will lose its control progressively. Additionally, increasing of anode chloride contents can increase macro-cell potential difference and decrease anode polarization slope but cannot affect cathode polarization slope, which means anode polarization resistance will be decreased and anode can generate enough electron for cathode to consume, and enlarging of macro-cell potential difference and decreasing of anode polarization slopes are the main reasons which escalate macro-cell current density dramatically.

### References

- [1] C.M. Hansson, A. Poursaeed, A. Laurent. Macrocell and microcell corrosion of steel in ordinary Portland cement and high performance concrete. *Cement and Concrete Research*, Vol.36,2006,pp.2098-2102
- [2] K. Soeda, T. Ichimura. Present state of Corrosion inhibitors in Japan. *Cement & Concrete Composites*, Vol.25,2003,pp.117-122
- [3] S. Miyazato, Y. Hasegawa. Proposal of Corrosion rate analytical model of reinforced concrete with crack. *Modelling of corroding concrete structures*, Vol.5,2011,pp.39-63
- [4] A. Neville. Chloride attack of reinforced concrete: an overview. *Materials and structures*, Vol.28,1995,pp.63-70
- [5] Verbeck, G.J. Mechanisms of corrosion in concrete, *Corrosion of Metals in Concrete*, Vol.49,1975,pp.21-38
- [6] T. Maruya, H. Takeda, K. Horiguchi, S. Koyama, K. Hsu. Simulation of Steel Corrosion in concrete based on the model of Macro-cell corrosion circuit. *Journal of Advanced Concrete Technology*, Vol.5, No.3, 2007, pp.343-362
- [7] Y. Ji, G. Zhan, Z. Tan, Y. Hu, F. Gao. Process control of reinforcement corrosion in concrete. Part 1: Effect of corrosion products. *Construction and Building Materials*, Vol.79,2015,pp.214-222
- [8] Ominda Nanayakkara, Yoshitaka Kato. Macro-cell corrosion in reinforcement of Concrete under Non-

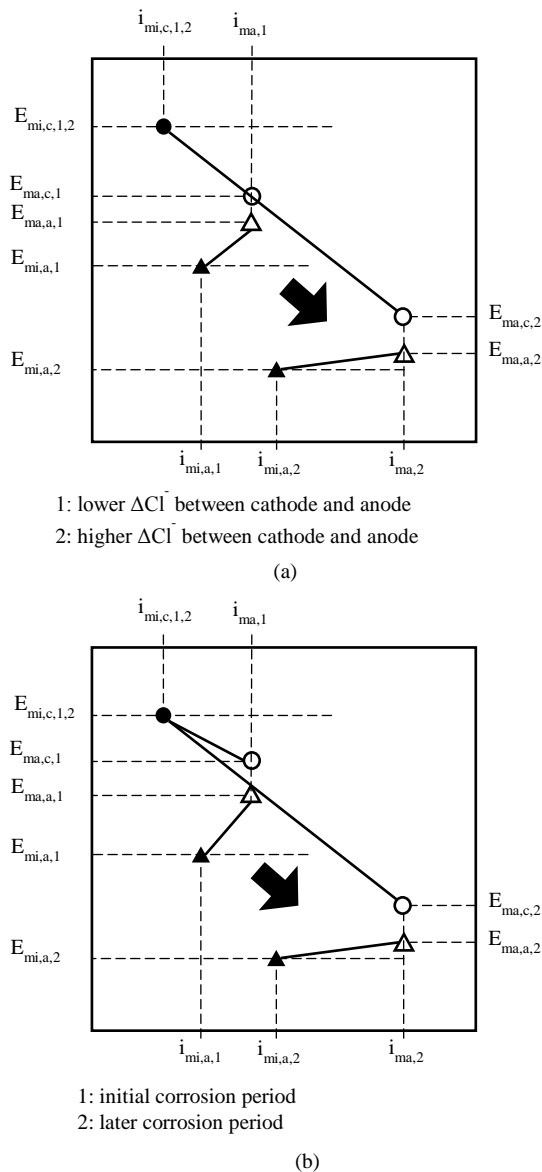


**Fig. 10** Corrosion mechanism in chloride-induced macro-cell corrosion

homogeneous Chloride environment. *Journal of Advanced Concrete Technology*, Vol.7, No.1, 2009, pp.31-40

[9] ASTM C876, Standard Test Method for Half-Cell Potentials of Uncoated Reinforcing Steel in Concrete.

[10] C. Alonso, C. Andrade. Corrosion of Steel reinforcement in carbonated mortar containing chlorides. *Advanced in cement research*, Vol.1, No.3, 1988, pp.155-163

[11] C. Andrade, J.A. Gonzalez. Quantitative measurement of corrosion rate of reinforcing steels embedded in concrete using polarization resistance measurements. *Materials and Corrosion*, Vol.29, No.8, 1978, pp.515-519

[12] N. Birbilis, B.W. Chery. Monitoring the corrosion and remediation of Reinforcement concrete on-site: An alternative approach. *Materials and Corrosion*, Vol.56, No.4, 2005, pp.237-243

**Gaozai Xu**, was born in Suzhou, Jiangsu Province, China in 1991. He is now a graduate student in Kyushu Institute of Technology (KIT) in Japan. His research concerns rebar corrosion.